Characterization of Optical Tweezers Potential using Scattering Techniques

A thesis submitted in partial fulfillment of the requirement
for the degree of Bachelor of Arts with Honors in
Physics from the College of William and Mary in Virginia,

by

Nicholas Everts Alford West

Accepted for _____
(Honors, High Honors, or Highest Honors)

_____
Director

_____

_____

_____

Williamsburg, Virginia
April 2001

Nicholas West

Advisor: Dr. W.E. Cooke

"Characterization of Optical Tweezers Potential using Scattering Techniques"

I. Abstract

This paper reports scattering of micro-spheres from the potential well created by optical tweezers. We explain how a trap is created and the forces involved. We present measurements of two-dimensional scattering, which allow the potential well to be characterized. We show that the results provide much more information than anticipated and that they even allow the development of a model that will predict future scattering behavior. We examine in detail how to determine and change the relative positions of the horizontal measurement plane and the laser focus so as to observe three-dimensional scattering.

II. Introduction

A. History

Optical tweezers, also called laser tweezers, were first devised by A. Ashkin[1] at Bell Telephone Laboratories in 1970. He used the radiation pressure of light to create a trap. To accomplish this, Ashkin used a focused laser beam to accelerate micron- sized translucent spheres suspended in liquids and gas, thus avoiding the perturbing thermal effects. At the time, Ashkin surmised that it would also be possible to use this technique to accelerate and trap atoms and molecules. In 1978, Ashkin achieved atom trapping by resonance radiation pressure. In the 1980's scientists discovered that this technique could be used to manipulate microscopic biological specimens such as viruses, bacteria[1], DNA[2] and sperm cells[3]. This technique has proved to be an important tool for the manipulation of cells in microbiology. In the 1990's optical tweezers proved to be useful for the measurement of small forces such as the force generation of organelle transport[1].

B. Theory overview

Laser tweezers rely on the radiation pressure of light. Light carries a momentum per photon $p = h / \lambda$, where h is Planck's constant and λ is the wavelength. When light passes through a translucent object, such as a piece of glass, it bends. This characteristic allows optical lenses to create an image at a specific point in space. A good example of this would be the

single lens reflex camera, which uses a system of lenses to image to a specially prepared medium, which records the incident light for posterity in the form of a photograph.

When the light bends, its momentum changes. Momentum is conservative, so this momentum change has to be made up. Therefore, the object that caused the light to change direction undergoes an equal and opposite change in momentum. This momentum change is felt as a force over time. Ordinarily, this force is negligible, but on the microscopic scale of a few microns, in liquid suspension, it becomes quite important. It can even be used to move small dielectric spheres or other translucent objects. The converging rays of light at the laser focus create a trap: transmitting objects are drawn by a restoring force towards the center. At equilibrium, the object rests at the center of the focus.

C. Purpose of project

The main thrust of this project is to accurately determine where the camera is imaging with respect to the laser trap and to be able to change this relationship. Then we can observe three-dimensional scattering, and hence be able to fully characterize the potential well. First, however, we must ascertain that we can observe scattering. Then we need to be able to record the scattering and analyze the data.

The final purpose and most important purpose of this project is to show that the scattering data can be used to measure the characteristics of the potential well created by laser tweezers. Then we can determine the forces within the trap and how they vary.

Once we have completely characterized the trap for this particular case, we can extend this technique to spheres of smaller dimension. Of particular interest is the case in which the spheres are of the order of a wavelength. In classical optics, there are two models for light. The Mie or ray optics regime applies to objects that are much bigger than the wavelength, while the electromagnetic wave regime applies to objects much smaller than a wavelength. The boundary between these two models is theoretically perplexing. Studying the case in which the sphere is of the order of a wavelength will allow insight into this problem.

D. Basic Optical Set-up

Our experimental apparatus consists of a 675nm, 30mW diode laser, two collimating lenses (L_1 and L_2) to correct the beam and make it more circular in cross section. The beam is steered by a mirror M_1 to a focusing lens L_3. From there, it goes to a dichroic mirror and is directed into the microscope body to the objective lens. The dichroic mirror has the special property of reflecting only red light incident at an angle of 45°, which allows us to image through the objective lens with a digital camera. The microscope has 4 lens magnifications: 3.5x, 10x, 40x and an oil immersion 100x lens. To adjust the focus we turn a knob, which moves the microscope stage up or down in relation to the objective lens. The fine focusing knob is graduated in microns and has a range of movement of 251 μm. The coarse focus knob moves the microscope stage vertically 1mm for every quarter turn.

III. Theory

A. Conservation of momentum

As briefly described above, light has momentum per photon equal to h/λ. When the light hits a reflective or refractive surface it undergoes a change in momentum. Because momentum of the system is conserved, the object receives an equal and opposite change in momentum.

Light rays "bounce off" of a totally reflecting object. Light obeys the laws of reflection, where the angle of incidence is equal to the angle of reflection. This angle is calculated from the normal to the surface. When light bounces off of the surface of an object, it loses momentum perpendicular to the surface. By conservation of momentum, the object gains momentum in the direction of the normal. Similarly, a fire hose can be used to push a small vehicle on a flat surface. The high-pressure jet of water loses momentum upon hitting the vehicle. Consequently, the vehicle gains momentum in the initial direction of the water jet: this is felt as a force, which causes the vehicle to move.

Light passing through a translucent object obeys Snell's law, given by $n_1\sin\theta_1 = n_2\sin\grave{e}_2$, where n_1 is the is the index of refraction of the first medium, n_2 is the index of refraction of the second medium, θ_1 is the angle of incidence of the light ray and $\grave{e}_2$ is the angle of refraction of the ray in the second medium (fig.1). The index of refraction is given by the ratio of the speed of light in a vacuum and the speed of light in the specific medium.
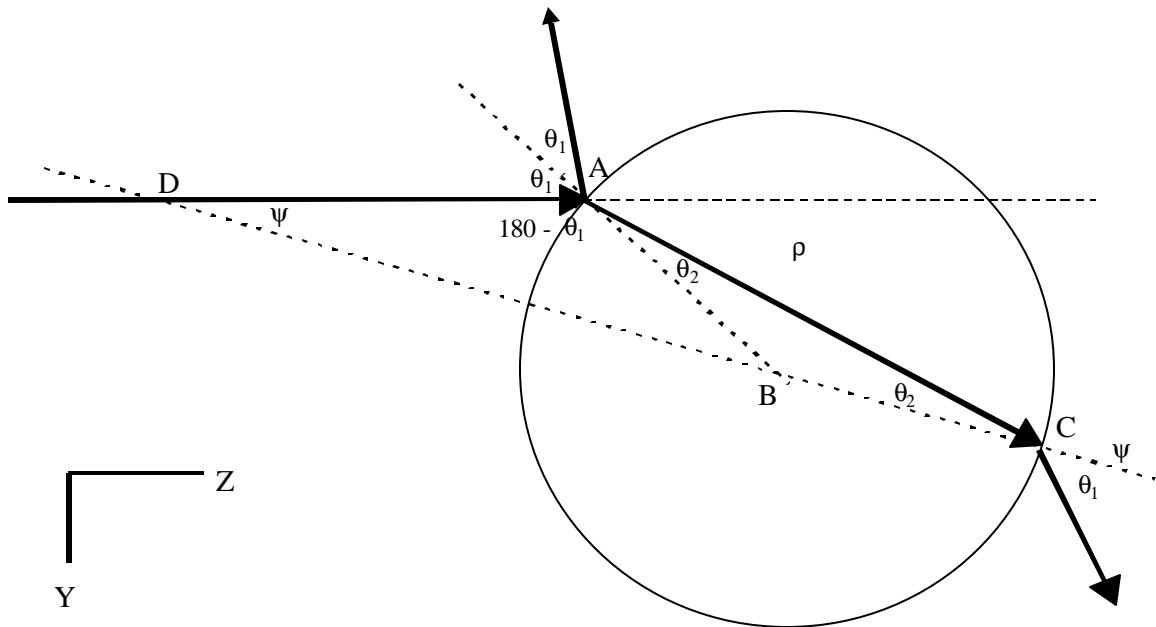

Figure 1: Geometry of a ray hitting a sphere.

Laser tweezers harness the momentum of light. When the ray enters a sphere it is reflected or refracted causing a change in direction of the incoming ray. This change in direction corresponds to a change in momentum. By conservation of momentum, the sphere gets an equal and opposite change in momentum. The sphere hence feels a force equal to the change in momentum per second. This is a repulsive force in the case of a totally reflecting sphere and a

restoring force in the case of the totally transmitting sphere. We will explain how this occurs in the next section.
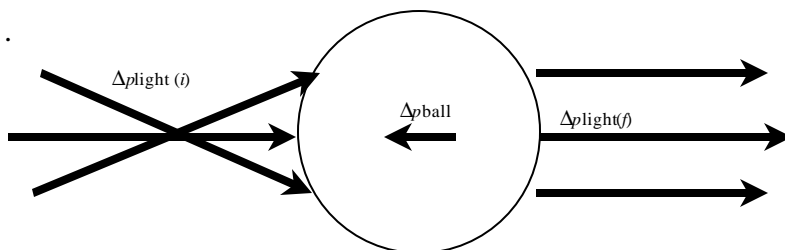
B. Trapping

1. When does it occur?

Trapping occurs when the incident velocity of the sphere is not enough to overcome the forces of the trap: consequently, the sphere is pulled into the center of the trap where it rests at equilibrium. In this instance, the sum of the forces is zero over the entire sphere. For the trap to be effective, the potential well must be deep enough to hold the sphere against perturbing forces such as the viscous and thermal forces. The following diagrams illustrate how trapping occurs.

a) Longitudinal trapping

Parallel rays going in the z direction hitting the sphere are bent or refracted: consequently, they converge to a point on the other side of the sphere. The sphere acts like a lens. The component of the light's momentum in the positive z direction is diminished when the rays are bent. Hence the ball must receive momentum in order to make up for this loss and conserve momentum. This momentum change is felt as a force over time.
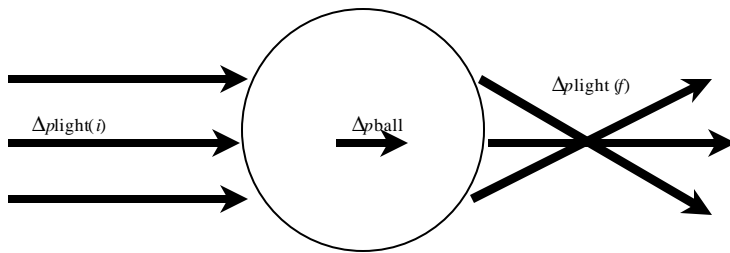

Sending in diverging rays, we get a rather unexpected result. Consequently, the exiting rays are parallel, following the principle of a thin lens. The component of momentum in the negative z direction is increased after passing through the ball. Hence, the ball receives momentum in the positive z direction in order to conserve momentum. This causes the ball to be pulled towards the incoming rays!

b) **Lateral trapping**

For transverse movement, we can model the sphere as a thin lens. As the lens is displaced downwards with respect to the incoming parallel rays, the light is bent downwards. The light gains a component of momentum in the negative y direction. To make up for this change, the lens gains momentum in the opposite direction. This is felt as a force in the positive y direction, which will restore the lens to its initial position.
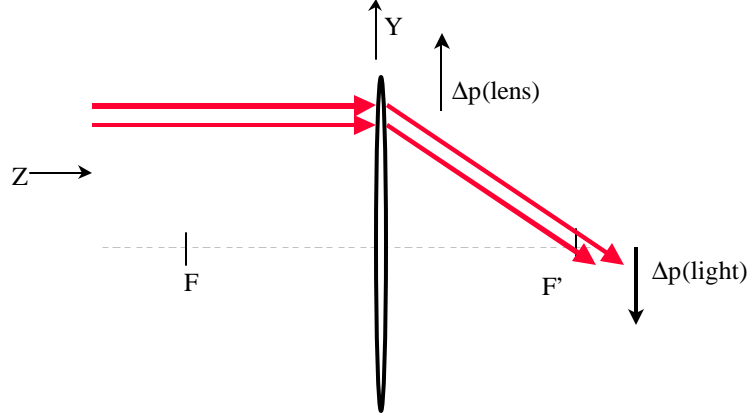
In all of these cases, the force felt by the object restores it to the equilibrium position, i.e. the focus of the laser beam.

2. Formalism for forces

Formally, we can separate the radiation force into two components defined by A. Ashkin[4]. The gradient force is perpendicular to the direction of the incoming laser beam, while the scattering force is in the direction of propagation of the beam. Ashkin gives the following equations of the scattering and gradient forces for a parallel incident ray on a sphere:

$$F_{scat} = \frac{n_1 P}{c} \left\{ 1 + R cos(2\theta_1) - \frac{T^2 [cos(2\theta_1 - 2\theta_2) + R cos(2\theta_1)]}{1 + R^2 + 2R cos(2\theta_2)} \right\} \qquad (1.1)$$

$$F_{grad} = \frac{n_1 P}{c} \left\{ R sin(2\theta_1) - \frac{T^2 [sin(2\theta_1 - 2\theta_2) + R sin(2\theta_1)]}{1 + R^2 + 2R cos(2\theta_2)} \right\} \qquad (1.2)$$

where P is the power of the ray, θ_1 is the angle between the incoming beam and the normal to the surface, θ_2 is the angle that the first transmitted ray makes with the perpendicular to the normal (fig.1). The $\frac{n_1 P}{c}$ term is the momentum per second transported by light of power P. R and T are the Fresnel coefficients of reflection and transmission, R is the fraction of the light

intensity reflected from the surface, T is the fraction of the light intensity transmitted through the surface. For polarization perpendicular to the plane of incidence, R and T are given by the equations:

$$R_P = \left(\frac{n_1 \cos q_1 - n_2 \cos q_2}{n_1 \cos q_1 + n_2 \cos q_2} \right)^2 \qquad (1.3)$$

$$T_P = 1 - R_P$$

where n_1 and n_2 are the indices of refraction.

For polarization parallel to the plane of incidence, R and T are:

$$R_S = \left(\frac{n_2 \cos q_1 - n_1 \cos q_2}{n_2 \cos q_1 + n_1 \cos q_2} \right)^2$$

$$T_S = 1 - R_S \qquad (1.4)$$

Calculating the forces and the Fresnel coefficients is straightforward for flat surfaces, however, it is much more complicated for a sphere: the angles of incidence change as the sphere moves through a beam of light. If the light rays are converging, the polarization of the light will depend on which surfaces the light is striking.

C. Scattering

1. Scattering from an attractive potential

When a ball is scattered from a potential, it changes its direction of motion. This direction change depends on where the ball is incident on the potential: to describe this incident trajectory, we define the scattering parameter of the ball. The scattering parameter is the perpendicular distance b from an axis traveling through the center of the potential (see figure 2). The ball is pulled towards the potential when it gets close enough. To visualize such a potential, let's imagine a trampoline with a heavy rock sitting on it. This causes the material to sag and create a "potential well". If we roll a ball near the edge of this dimple, we will observe a deflection in the ball's trajectory as it rolls past and is drawn towards the center of the indentation. If the velocity that we give the ball is not sufficient, the ball will become stuck in the well: it is "trapped". If however, the initial trajectory of the ball does not take it close enough to the well (i.e. the scattering parameter is too big), there will be no effect: the ball will not be deflected. If we can imagine that we remove the rock and still have the indentation in the fabric, we can imagine sending the ball through the center regions of the well. The ball will be most

deflected for scattering parameters just smaller than the radius of the well. If we send the ball through the center of the well there will be no deflection. However, there will be a change in the velocity of the ball: the ball will speed up as it rolls down into the indentation and will slow down as it rolls uphill out of the indentation.

2. Scattering in a viscous medium

In a viscous medium, the objects in motion experience a viscous force, contrary to the direction of motion. When an object is scattered, it slows to a stop after deflection (Fig 2). To make this more apparent, let's imagine that we have our trampoline again. The indentation now stays in the same place relative to the ground no matter how we move the trampoline parallel to the ground. The trampoline fabric is covered with honey, which causes the ball to stick to the surface. As we move the trampoline surface with the ball sitting on it such that the ball passes through the indentation, we would see the following: the ball will be drawn towards the center of the indentation and roll backwards slowly as it re-emerges from the "well". The honey in this example gives us a viscous force. It causes the ball to not move as freely. The balls deflection is minimized because the honey cases it to slow to a stop. As it exits the trap, the honey actually keeps the ball from rolling all the way back into the trap and getting stuck or trapped. This example can be applied to this particular experiment: We have a glass slide, analogous to the trampoline surface, which is covered with water (analogous to the honey).
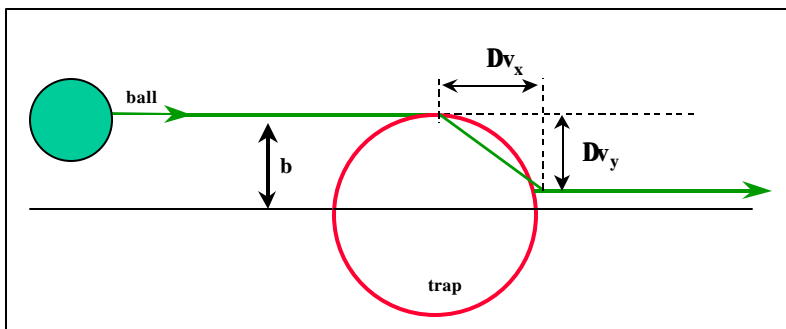

Figure 2: Diagram showing a ball scattering from the trap or attractive potential at an impact parameter b. The ball undergoes velocity changes in the x and y directions, $\ll v_x$ and $\ll v_y$, due to the forces of the trap.

IV. Criteria for observation of scattering

A. Trap characteristics

1. Power through lens

If the lens is under-filled, the effective NA rating of the lens will be reduced: the trap won't be as well focused or as intense. If, however, it is overfilled, there will be some power loss and the trap won't be as strong. It is therefore best to just slightly overfill the lens. In that interest, we modified the set-up to benefit the power through-put of our lens of choice. We removed the doubling telescope assembly, which decreased the beam waist to 2.5mm. The

power jumped from 4mW to 12mW at the objective, a very significant increase. Not only had the overfilling been reduced, but the number of surfaces that the beam goes through was reduced, which also contributed to the power gain. Each glass surface reflects 4% of the incident light. After this, the balls were pulled into the trap with much more alacrity: the trap seemed to be stronger.

2. Lateral dimensions of trap

The laser beam never actually focuses to a point, but reaches a minimum waist given by $w_0 = 0.61 \lambda/NA$. The waist is the radius of a beam and serves as a good indicator of spot size. As the numerical aperture gets bigger, the minimum spot size gets smaller. Since the trap is small in comparison with the ball size, we can't get a detailed reading of the characteristics of the trap (Fig.10).

lens	NA	w_0 (mm)
10X	0.25	1.65
40X	0.65	0.63
100X	1.3	0.32

Figure 10. Table showing the lateral dimensions of the trap for three lenses (for $\lambda = 675$ nm)

B. Viscous drag force

The viscous drag force in a medium of viscosity η is given by Stokes equation:

$$F_d = -6\pi\eta r_b v_b$$

where r_b is the radius of the ball and v_b is the velocity of the ball. As the velocity of the ball increases, the viscous drag force increases proportionately. The drag force is also proportional to the radius of the ball. For a ball of radius 5μm, travelling in water of viscosity $\eta = 10^{-3}$ N s / m^2 at a velocity of 54 μm/sec, the drag force is 5 pN. We know that

$$F_d = m_b a = m_b \frac{dv_b}{dt}$$

where a is the acceleration of the ball due to drag force. Solving this for v_b, we get the equation:

$$v_b = v_0 e^{\frac{-t}{\tau}} + v_{terminal}$$

where the time constant $\tau = \dfrac{m_b}{6\pi\eta r_b}$

Because the ball has a small mass ($m_b = 5.5 \times 10^{-10}$ g), τ is very small: $\tau = 5.8 \times 10^{-6}$ seconds. This is instantaneous compared to the time between video frames of 3.3×10^{-2} seconds. This means that the any velocity greater than the terminal velocity damps out instantaneously. Hence, the ball is always at terminal velocity if it is moving relative to the fluid. This fact has far reaching implications.

We must remember that the ball is at rest in the reference frame of the stage until it falls

under the influence of the trap whereupon it moves relative to the fluid, which is at rest in the reference frame of the stage.. Since the ball can never move faster than terminal velocity if it is moving relative to the fluid, the viscous drag force must always exactly oppose the forces of the trap. Hence $F_{trap} = F_d$, and we can write:

$$F_{trap} = 6\pi\eta r_b v_{terminal}$$

or to put it another way,

$$F_{trap} = \frac{m_b}{t} v_{terminal}$$

The viscous force plays a crucial role in the measurement of the forces of the trap as will be seen below.

C. Technical considerations

One thing that we need to take into consideration is the fact that the video recorder captures at 30 frames per second. This means that the ball can't be moving too fast because some important data will be lost between frames.

Pixel resolution is limited by the translation process from the video cassette to the avi file: any resolution higher than 120x160 results in more than 10% of the frames being dropped in the translation.

Also we are moving the stage laterally by hand: the velocity variation shouldn't be too great over the small distances we are moving the ball (approx. 100μm). However on examination of the data, we found that the stage underwent a short hesitation defined by de-acceleration followed by an acceleration: a possible explanation could be an imperfection in the gearing of the translation mechanism, such as a worn gear tooth (see figure 14).

One other consideration is the tendency of the spheres to stick to surfaces. David Leichtman also mentioned this problem. To characterize scattering in three dimensions, we need a sphere floating freely in the body of the solution. That way we can look above and below the scattering candidate. Once the spheres reach the bottom, they have a tendency to stick. We found that by agitating the slide or turning it upside down for a few minutes, we could bring the balls back into free suspension. When the slide had been left alone for a few days we found that some water had evaporated and that most of the spheres were stuck. We rectified this problem by using an eye-dropper tip to dislodge the spheres (any hard, pointed object will suffice).

V. Exploring the third dimension

A. Determining and changing the relative positions of the laser spot

and the measurement plane

1. Using the slide reflection

In order to characterize trapping in three dimensions, we first need to understand how our apparatus works in three dimensions, namely how to determine the relative positions of the digital camera focus plane and the laser trap focus. This is important because we want to be able to move the camera focus plane above and below the laser spot: by doing this, we can examine scattering as it occurs above and below the trap. If the camera focus plane is above the trap and we see a ball come into focus as it enters the trap we will know that it got deflected upward by the trap forces. By studying the deflection, we can characterize the forces of the trap in the longitudinal direction. Previous work did not explore this problem in depth.

To make these measurements, we employed a 1.2mm thick glass slide placed on the microscope stage. We then looked for the reflection of the laser spot off the top and bottom surfaces of the slide imaged to the camera. Moving the microscope stage up or down using the micron-graduated knob, we could focus the camera on the top or bottom surface of the slide (marked with a grease pencil). Ray tracing diagrams indicated that we would have to take into account the fact that the laser spot was being reflected.

2. Zero point

We call the position at which the laser spot is in the same horizontal plane as the CCD camera focus the "zero point": this is when the laser spot and the slide surface are simultaneously imaged on the t.v. screen. We define L as the distance from the camera to the objective and x_0 as the distance from the slide surface to the objective (Fig. 3).
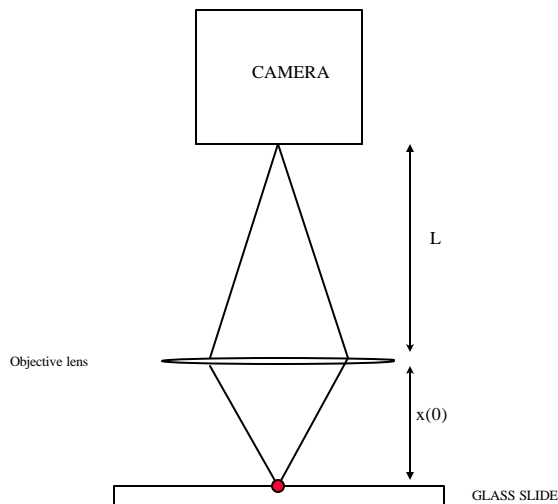

Fig. 3 The camera at the "zero point"

3. Case of camera focus plane below laser spot

When we move the camera down, the focus plane is below the laser spot. We no longer see the laser spot and the slide surface on the t.v. screen at the same time. As we bring the focus in, we see the slide surface followed by the laser spot. At first glance, we would say

that the movement of the microscope stage was a straight-forward way to determine distances between imaged objects. However, we must take into account the fact that the glass slide acts like a plane mirror. The image observed on the t.v. screen is actually the virtual image of the laser spot seen in the slide. In the same way, when we look into a bathroom mirror, we see a reflected image of ourselves. This image is located behind the mirror, twice the distance from us to the mirror surface. The image that we see is situated in virtual space and is called a virtual image because it is not physically located behind the mirror surface. If we were to focus a single lens reflex camera at our image in the bathroom mirror, moving the focus from its closest point towards infinity, we would first see the cracks on the surface of the mirror followed by the image of ourselves (analogous to the image of the laser spot).
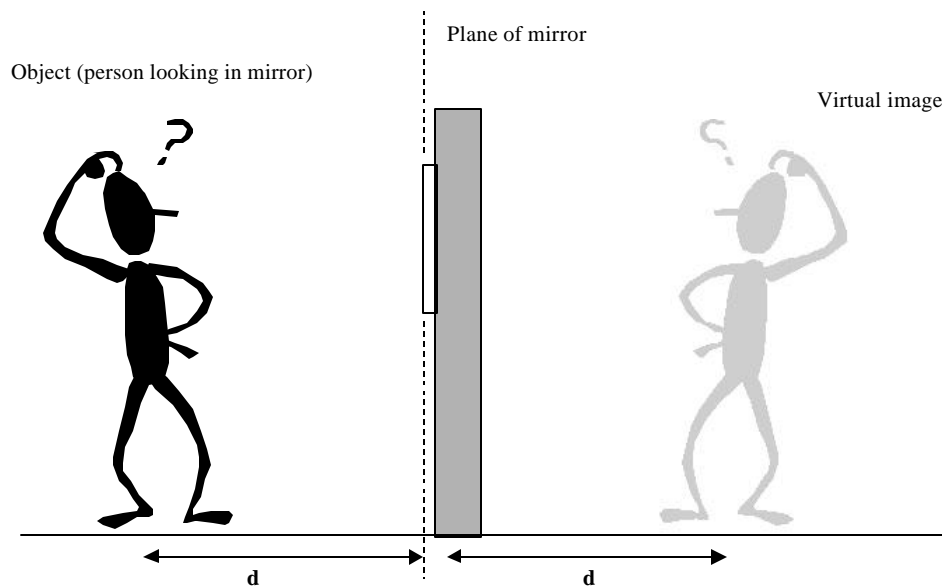

Figure : A person looking in the bathroom mirror at a distance d from the surface plane of the mirror sees his virtual image in the mirror. The virtual image appears to be a distance d behind the plane of the mirror.

To make the analogy as close as possible, let's imagine that the wall on which the mirror is fixed is movable (like the microscope stage). Now suppose we focus on our image in the mirror. Keeping the focus fixed, the wall is moved away from us until the surface of the mirror comes into focus. We would observe that the distance from ourselves to the mirror was double what it originally was (see Figure ?). If we were to approach this casually (barring the fact that we know where we are located physically), we might be tempted to say that the distance between this person in the mirror and the surface of the mirror was the distance that the wall moved: at the initial position of the wall, we saw a person and at the final position we saw the surface of the mirror. However, we know quite well that we were not focused on a real physical person situated in real space because this would be physically impossible, not to say logically impossible!
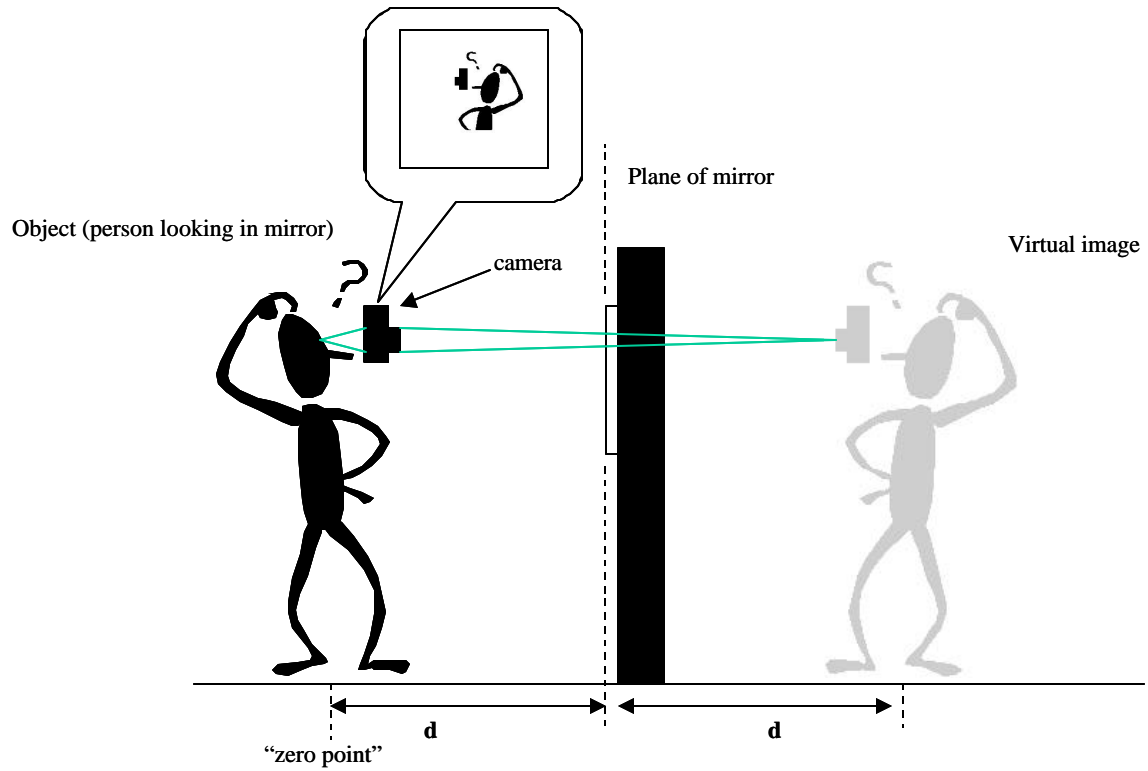
Figure : A person focusing with a camera on his image in the mirror. He observes his image in the viewfinder of the camera. He is situated a distance d from the mirror and an optical distance 2d from his virtual image situated in the behind the mirror. The camera is focused to a position in space a distance 2d from the lens. We will call the person's position the "zero point"(this is to make the analogy more apparent (see figure).
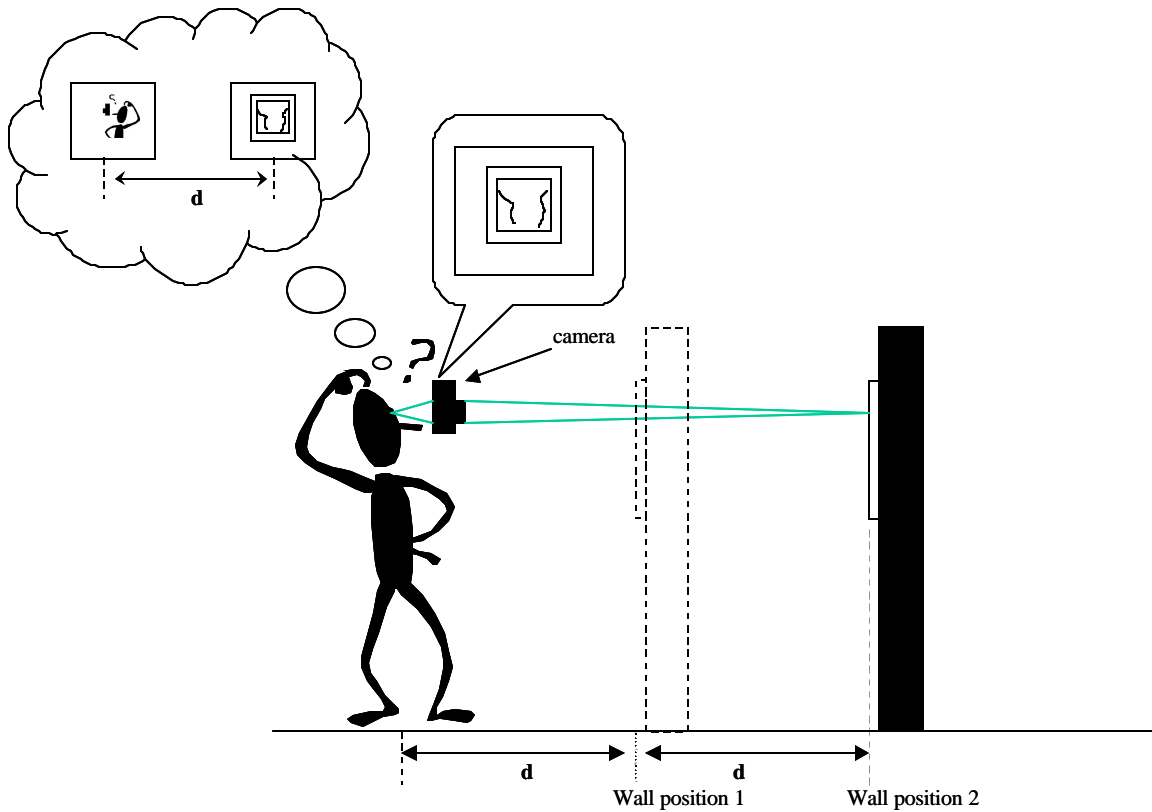
Figure : At the second position of the wall, the person will observe the surface of the mirror itself through the viewfinder of the camera. To a casual observer the physical distance between the person and the surface of the mirror is equal to the distance d traveled by the wall in order to get from the first image (wall position 1) to the second image (wall position 2). This is quite obviously false.

Similarly, in our set-up, to go from imaging the laser spot to imaging the slide surface, we have to move the slide away from the initial position to twice the original distance from the physical position of the laser spot (which is analogous to our physical position in the bathroom of the previous example). The initial position of the slide is situated halfway between the real position of the laser spot and the camera focus plane The position of the laser spot never changes: at the "zero point" the top surface of the slide is located in the same horizontal plane as the laser spot (see fig. 3). In other words, using the slide reflection, the observed distance x_i^L between the spot and the slide surface is half the true distance x_i^p. Hence, the real distance between the focii is in actuality double the measured value (fig.4).
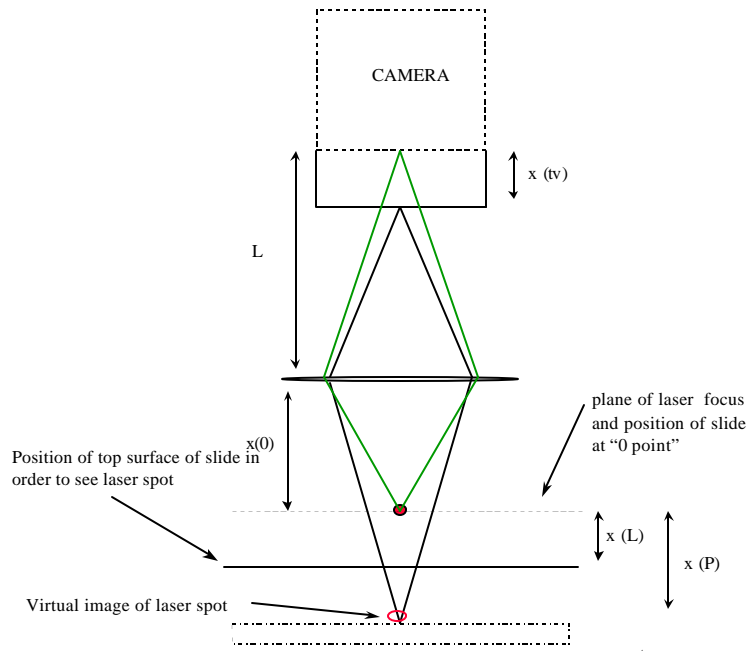
CAMERA

x (tv)

L

x(0)

Position of top surface of slide in
order to see laser spot

plane of laser focus
and position of slide
at "0 point"

x (L)

x (P)

Virtual image of laser spot

Figure 4: Case in which camera is moved down a distance x_i^{tv} from the "zero point".

4. Case of camera focus plane above laser spot

When we move the camera up from its position at the "zero point", the camera focus
plane is positioned above the laser spot. Moving the camera focus in from afar, we see the laser
spot followed by the slide surface. This time, the spot observed on the t.v. screen is the actual
spot reflected up off the surface of the glass. In this case, the image of the spot only becomes
visible when the reflected spot is physically in the same plane as the camera focus. This occurs
when top surface of the slide is positioned halfway between the horizontal camera focus plane
and the horizontal plane containing the laser spot (fig. 5). Again we find of a factor of two
difference between the observed distance of the foci and the real distance. The distance of the
stage x_i^L from the "zero point" in order to view the laser spot is half the distance of the stage in
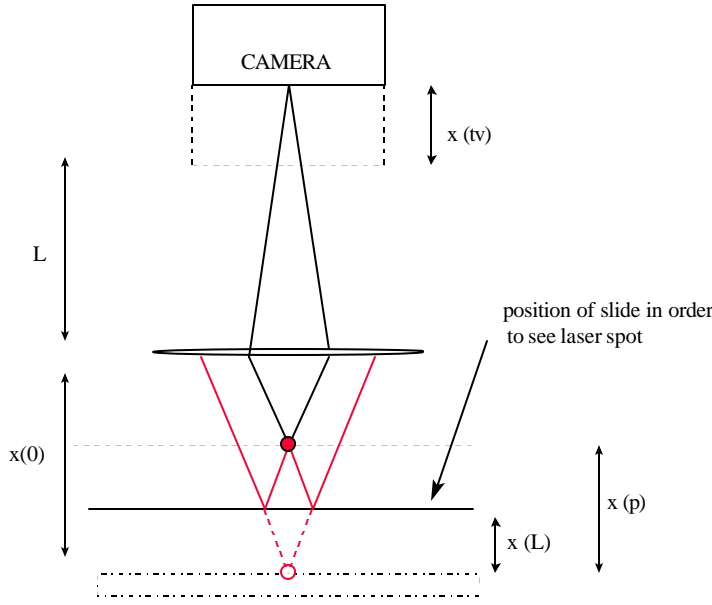order to see the slide surface

Figure 5: Case in which camera is moved up a distance x_i^{tv} from the "zero point".

B. The thin lens model

1. Formalism

Writing down the thin lens equation for the camera focus and the laser focus $1/f$ $=1/d_o+1/d_i$, where f is the focal length, d_o is the distance lens-object and d_i is the distance lens-image, helped us understand the effect of moving the camera on the relative positions of the focii. For the surface of the slide to imaged, the thin lens equation is:

$$\frac{1}{f} = \frac{1}{L + x_i^{tv}} + \frac{1}{x_0 + x_i^{p}} \qquad (1.3)$$

where f is the focal length of the lens, L is the distance from the objective lens to the camera at the "0 point", the point at which the laser spot and the camera focus occupy the same horizontal plane. x_0 is the distance between the lens and the slide surface at the "0 point", x_i^{tv} is the vertical movement of the camera and x_i^{p} is the measured stage movement from the "0 point" to image the surface of the slide.

For the laser spot to be imaged, the thin lens equation is:

$$\frac{1}{f} = \frac{1}{L + x_i^{tv}} + \frac{1}{x_0 + 2x_i^{L}} \qquad (1.4)$$

where x_i^{L} is the movement of the stage from the "0 point" in order to view the laser spot. The factor of 2 in front of the x_i^{L} term corrects for the fact that the slide surface acts as a plane mirror (figs 2,3).

Equations 1.3 and 1.4 imply:

16

$$2x_i^{\,L} = x_i^{\,p} \qquad\qquad\qquad (1.5)$$

which we verify experimentally.

2. Measurements of slide surface and laser spot positions

For different camera positions, we took measurements of the absolute stage movement from the "zero point" position in order to image the laser spot and to image the top surface of the slide. As before, for each camera position x_i^{tv}, we define x_i^L as the distance from the "zero point" to image the laser spot and x_i^p as the distance from the "zero point" to image the top surface of the slide. At the "zero point" both laser spot and t.v. focus are at the top surface of the slide. These measurements gave us a relationship between the camera focus movement and the laser spot focus movement, that, in fact, as predicted, the camera focus always moved twice that of the laser spot due to the reflection off of the slide (Figs. 6,7). Again, the real position of the trap without the slide is twice the distance measured.

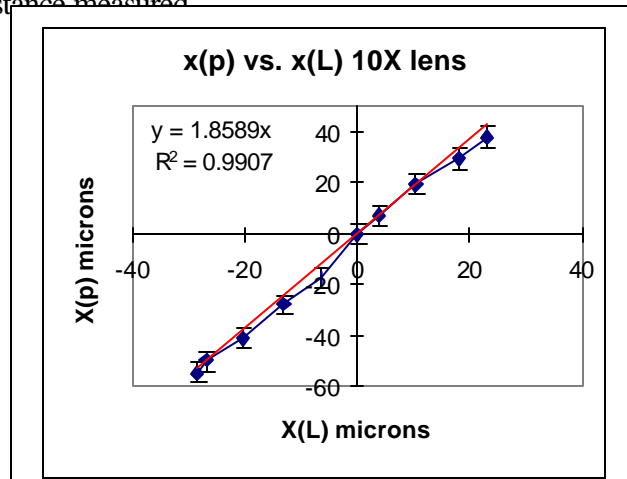| x(L) (microns)	x(p) (microns)
-28.5	-54.5
-27	-50
-20.5	-41
-13	-28
-6.5	-17.5
0	0
4	7
10.5	19.5
18	29.5
23	38

Figure 6: Stage movement x_i^p to view the slide surface vs. stage movement x_i^L to view the laser spot for the 10X lens. Notice that the relationship tallies with our prediction (1.5) within experimental error.

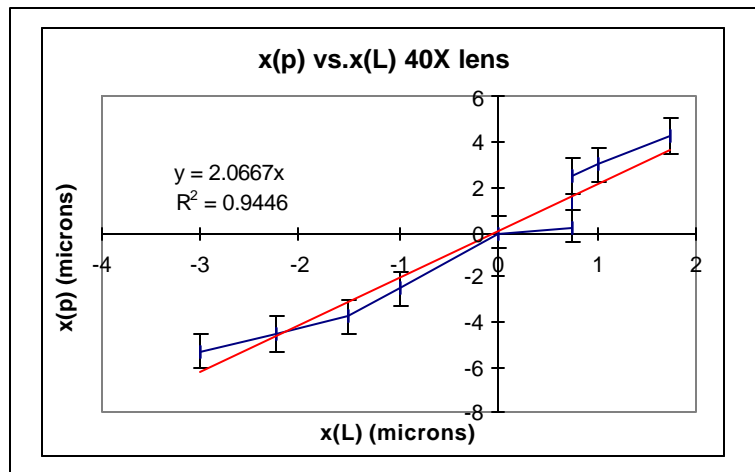| x(L) (microns)	x(p) (microns)
-3	-5.25
-2.25	-4.5
-1.5	-3.75
-1	-2.5
0	0
0.75	0.25
0.75	2.5
1	3
1.75	4.25

Figure 7: Stage movement x_i^p to view and to view the slide surface vs. stage movement x_i^L to view the laser spot for the 40X lens. Notice that the relationship tallies with our prediction (1.5) within experimental error.

C. Observe scattering in 3-d?

1. Characteristics of the lenses

As the focal length of the lens decreases (i.e. magnification increases), the range of stage movement decreases with camera movement. Hence at higher magnifications, the vertical range of motion is reduced. One concern that this brings up is whether the camera focus can be moved beyond the vertical limits of the trap. The Raleigh range, a measure of tightness of focus, gives us a reasonable idea of the longitudinal dimensions of the trap. In order to examine scattering in three dimensions, we wish to be able to move our camera image plane above and below the trap. We found that the 10X and 40X lenses obeyed the thin lens equation. The relationship between the camera position and the corresponding slide position is linear for small changes (fig. 8). This linear approximation gives us the following equation:

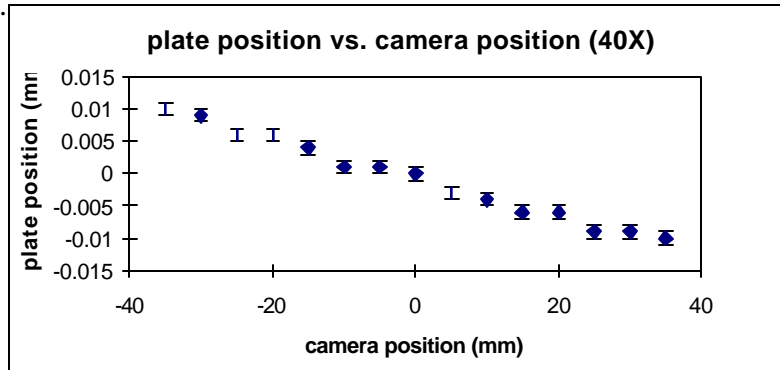$$x_i^{\,p} \approx \left(\frac{x_0 - f}{f} \right)^2 x_i^{\,tv}$$

Figure 8: Measured values showing the how camera focus plane movement affects the focusing range. The camera's range of 7cm allows the focus plane position to change by 20μm. The plate position measurement error is ± 1μm.

2. Raleigh range

The Raleigh range is defined as the distance from the where the focused laser beam is narrowest with a waist w_0 to the point where it is $2w_0$ (Figure). The Raleigh range z_0 is given by the equation:

$$z_0 = \frac{\boldsymbol{p} w_0^{\,2}}{\boldsymbol{1}} \tag{1.7}$$

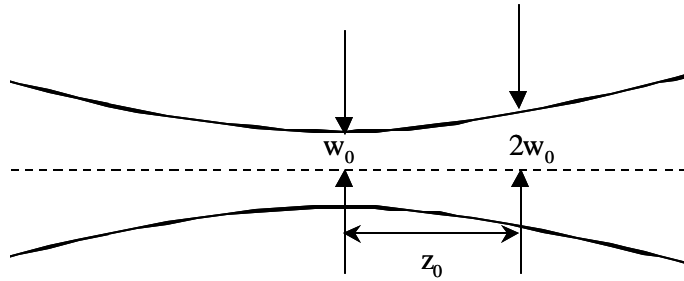where λ is the wavelength.

Figure : The Raleigh range z_0 is the distance for a Gaussian beam to increase from the minimum beam waist of w_0 to a beam waist of $2w_0$. (A focused beam never focuses to a point).

The divergence angle of the beam can be approximated by:

$$\tan\boldsymbol{q} \approx \frac{w_0}{z_0} \qquad (1.8)$$

Using these expressions and that at for small angle θ, $\tan\theta \approx \sin\theta$ we can write:

$$z_0 \approx \frac{\boldsymbol{l}n^2}{\boldsymbol{p}(NA)^2} \qquad (1.9)$$

where $NA = n\ sinu$ is the numerical aperture of the microscope objective. n is the index of refraction of the medium and u is the half-angle of the focused cone of light (see figure). The Raleigh range will change for different indices of refraction.
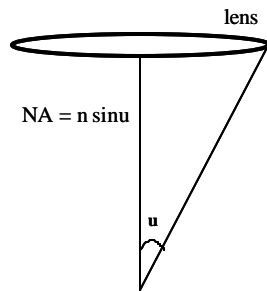

Figure : The numerical aperture (NA) is a measure of a lens's ability to resolve two points separated by a certain distance: the bigger the NA, the smaller the distance between two just resolvable points. If the diameter of a beam entering a lens is less than the lens diameter we say that the lens is under-filled: the maximum half angle u of the focused cone of light is reduced.
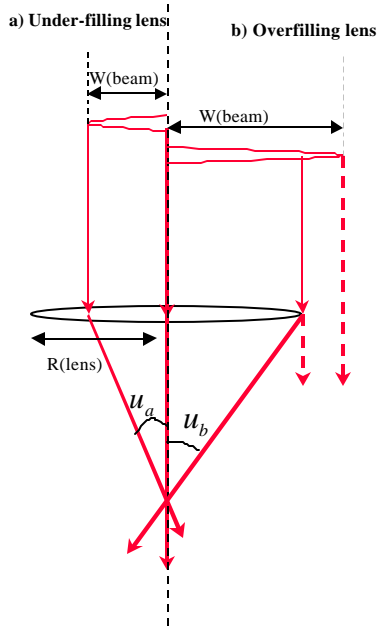
Figure : a) Under filling the lens means that the waist of the incoming beam w_{beam} is smaller than the radius of the of the lens R_{lens}. This has the effect of reducing the effective NA by reducing the maximum half angle of the focused rays u_a. b) Overfilling the lens means that the beam waist w_{beam} is bigger than the radius of the lens R_{lens}: some of the beam does not even go through the lens resulting in power loss of the focused beam. The half angle of the focused cone of light u_b is the maximum allowed by the radius of the lens: hence the NA is the maximum allowed in a medium refractive index n.

lens	NA	f (mm)	z_0 (μm)	max. x_i^p (μm)
10X	0.25	16	5.75	± 175
40X	0.65	4	0.85	± 10 *
100X	1.3	1.6	0.22	± 1

Figure 9: Table showing calculated Raleigh range z_0 and the range of movement about the laser spot x_i^p for a camera movement x_i^{tv} of ± 35 mm (we assume that the 100X lens obeys the thin lens equation). We are using a combined refractive index of n=1.3 of the glass cover-slide and the solution to get the Raleigh range.
* measured value (see fig. 8)

3. Choosing a lens

From the table (fig. 9), we can see that we should be able to observe scattering beyond the limits of the trap in the longitudinal direction for all the lenses and that in fact, the dimensions of the spheres are significantly greater than those of the trap. The best lens for our purposes seems to be the 40x lens because it allows a greater range of travel in the vertical direction while still allowing trapping and scattering to be observed.
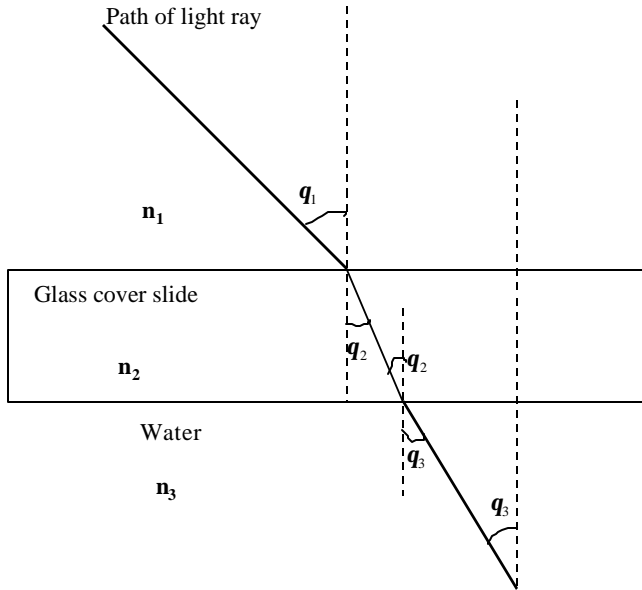
Figure : Ray tracing diagram showing a single ray from the laser going through the glass cover-slide ($n_2 = 1.5$) into the water solution ($n_3 = 1.33$) in which the balls are suspended. The first medium is air ($n_1 = 1$). For the 40X lens, Snell's law gives $\theta_1 = 40.5°$, $\theta_2 = 25.7°$ and $\theta_3 = 29.3°$.

One other thing to keep in mind is the enormous size of the ball compared to all dimensions of the trap (see discussion above). Figure shows that we need to consider the fact that parts of the ball will intersect the focused beam before it enters the focus itself. This has for effect of increasing the apparent lateral size of the trap. Using geometry we can determine the distance that the ball is from the center when its edges are tangential to the outermost rays.

1) The right triangles ABD and AOB are similar.

2) Hence angles ABD and AOB are equal. We will call this angle θ_3 (for the 40X lens $\theta_3 = 29.3°$ see above).

3) $\cos(AOB) = \cos(\theta_3) = R/OB$

4) Hence $OB = R/\cos(\theta_3) = 5.73\ \mu m$.

5) Since $R = 5\mu m$, the edge of the ball is $0.73\mu m$ from the center of the focus. The apparent lateral radius of the trap is $0.73\ \mu m$ (compared to $0.63\mu m$)
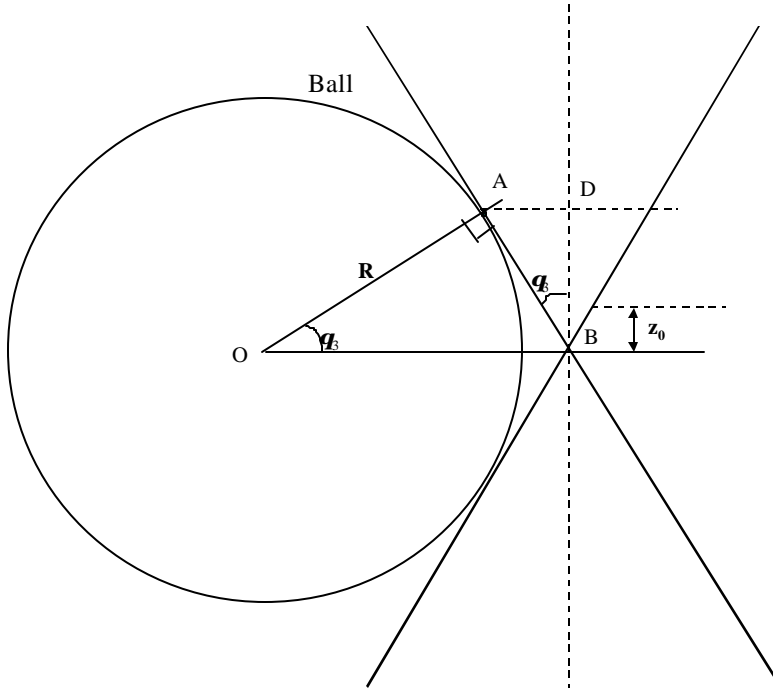
Figure : Diagram showing the ball and the beam focus (we are approximating the focus as a point compared to the ball size). Shown is the effective Raleigh range $z_0 = 0.85$ μm to scale with the ball of radius R =5μm. This diagram also illustrates that the ball should enter the focused beam before it actually enters the focus itself (at point B). This has for effect of making the apparent beam waist larger.

VII. Experimental methods

A. Equipment and set-up details

The apparatus consists of a Leitz Wetzlar microsope body with 4 lenses: 3.5X, 10X, 40X and a 100X oil immersion lens which image to a digital camera. The camera is a Schumberger CCD camera connected with BNC cables to a t.v. monitor. The laser is situated 40mm away from the first collimating lens L_1. The collimating lenses L_1 and L_2 are positioned 70mm apart. The focusing lens is positioned approximately 260mm from the dichroic mirror. The focusing lens has a focal length of 160mm. Thus, at the "zero point", camera is situated approximately 100mm from the dichroic mirror. The beam waist is approximately 2.5mm, which allows the 40X lens to be slightly overfilled. At the "zero point" for the 40X lens the camera-objective distance L is approximately 190mm. This makes the beam waist at the objective approximately 3mm. The diameter D of the lens we calculate to be 5.2mm. The lens is overfilled since the diameter of the beam is around 6mm.
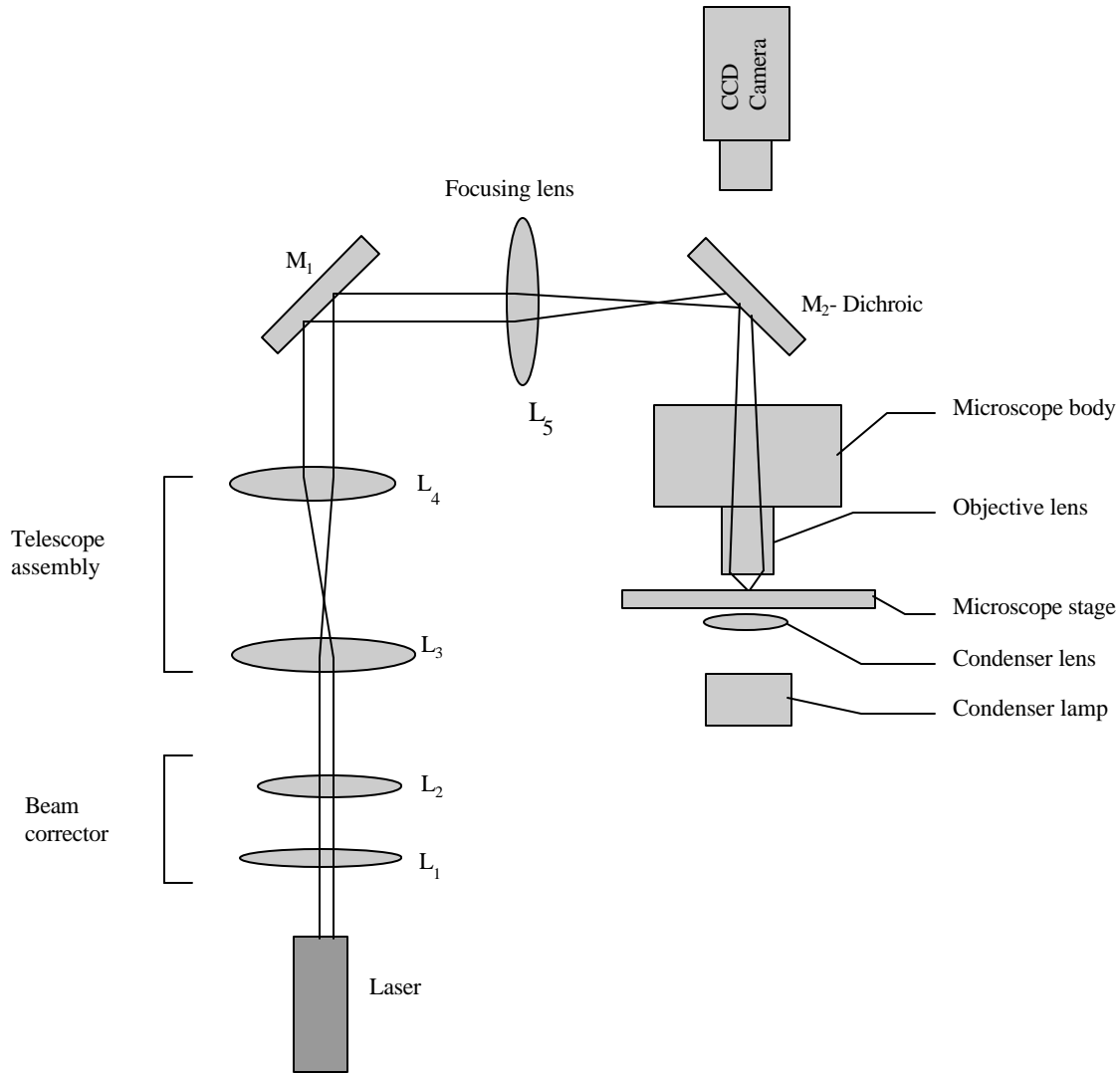
CCD Camera

Focusing lens

M₁

M_2- Dichroic

Microscope body

L_5

Objective lens

L_4

Telescope assembly

Microscope stage

L_3

Condenser lens

Condenser lamp

Beam corrector

L_2

L_1

Laser

Figure 11: the experimental set-up

B. Taking measurements

In preparation for our scattering experiment, we fill a glass well slide with several drops of water. We then add a drop of the microsphere solution (Polybead® polystyrene 10μm microspheres, Polysciences, Inc.). We use a cover slip to seal off the well. This relatively deep well (≈ 260 μm) allows us more time for the experiment because the spheres take longer to settle to the bottom under the influence of gravity. In order to record the scattering, we use a VHS video recorder running in SP mode, giving us a capture rate of 30 frames per second. With the tape running, we translate the stage laterally. We make several passes, allowing our candidate sphere to pass the trap at various scattering parameters and velocities. We transfer the footage to an ".avi" file using Microsoft AVREC Capture Tool software. We then use an Excel macro program written by the author to analyze the data. One thing to keep in mind is that the sphere is at rest in the reference frame of the stage until it feels the forces of the potential well.

The Excel program allows us to view the scattering footage and measure the position of the ball frame by frame. We found the appearance of a deposit on the slide surface very useful as a reference point to compare the stage movement to the ball movement. The Excel macro gives us the position of the ball in pixels. Therefore we need to translate these measurements into microns. We first used the 40X lens to note the position of the ball at each edge of the t.v. screen using the stage translation vernier. However we found this to be too imprecise (error $\pm$ 25%). The stage translation vernier is graduated in tenths of a millimeter, while we want to measure distances within at least 10 microns. We achieved better precision with the 3.5X lens. This lens has a bigger field of view, which allows a greater distance to be covered, thus minimizing the error. With this method we achieved a calibration precision of 3% or better. Scaling our result up for the 40X lens, we found that 1 pixel translated to approximately 0.31 μm.

VIII. Results

A. Evidence of Scattering

The captured video proves that we can observe scattering in two dimensions. We can measure the forces of the trap in function of the position of the ball.
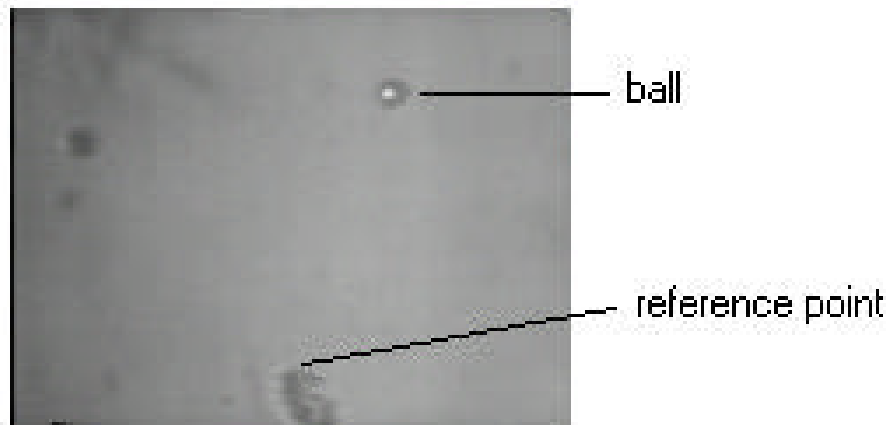

Figure : A frame showing what we saw on the t.v. monitor: the 10μm ball and the deposit on the well slide which served as a reference point since it never moved with respect to the stage.
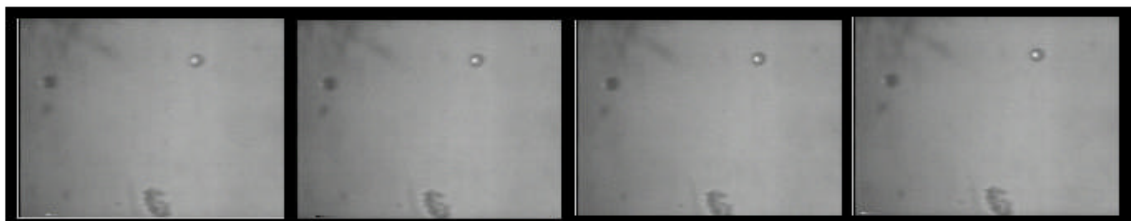

Figure : Captured video sequence showing the scattering event (frames 174-177).

B. Data

1. Measurements

Plotting position versus time for the x and y coordinates, we gain a fuller understanding of the scattering event. Figure 12 shows the scattering event in the reference frame of the stage for both x and y coordinates versus frame number. The frames are spaced at 1/30 second increments. The y coordinates of the ball show the abrupt deflection of the ball as it is pulled into the trap (frames 174-177). The x coordinates show that the ball slows down once the y forces have pulled the ball into the trap. Notice the offset between the y and x velocity changes: the velocity loss of the ball in the x direction occurs after the y deflection has taken place (frame177). This is a very important feature as far as understanding the behavior of the ball in the potential, with implications that will be explained by our model. The ball is pulled into the trap where forces in the x direction take precedence (frames 177-181): as the stage continues to move past the trap, the viscous forces drag the ball away from the trap and the ball regains the velocity of the stage on which it is resting.
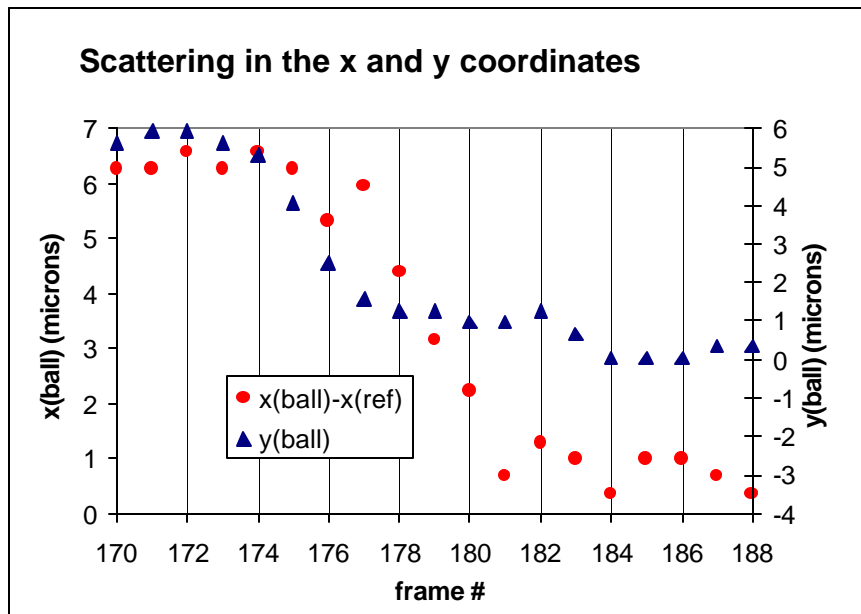

Figure 12: Scattering in the x and y directions in the reference frame of the stage versus the frame number. (We subtracted the x coordinates of the reference from the x coordinates of the ball to eliminate the x translation movement of the stage).

We determined the average velocity in the x direction of the stage by performing a linear fit to the data points (Figure 13, in blue). This fit was good with an R^2 value of 0.9953 (1 is a perfect fit while 0 means that the points fitted have no semblance to a line). This gave us an average stage velocity of 1.8 μm/ frame or 54μm /sec. However, when we subtracted the linear

approximated values from the measured values, we found some periodic non-random variations from the approximation, which seem to suggest that the stage translation was not functioning smoothly (Figure 14, in blue). The stage did not move in a linear fashion (see section IV C)). For frames 164 –189, the variance of the measured x positions of the reference point from the linear approximation of the stage translation was ± 1 μm. This gives an uncertainty in the velocity prediction of the stage of ±1.4 μm/frame! This is due to the large non random variations in stage movement which are not errors in measurement but are due to a less than perfect approximation of the non-linear translation of the stage. In order to ameliorate this approximation and get a better measure of the average velocity of the stage we notice that the biggest variation from this mean occurs just before the scattering event (frames 168-173): fitting a line to frames 173 to 188 we split the variance in half from the previous fit and get a average stage velocity of 1.7 μm/frame for this time period. Unfortunately due to time constraints we are not able to make the all the graphs reflect the slightly revised initial velocity of the stage and hence the ball. To correct for the stage "jitter" and to get a more realistic evaluation of our experimental error, we subtract the reference x coordinates from the ball x position, point by point, which gives an error of approximately ± 0.4 μm. Assuming comparable errors in the measurement of the x coordinates of the stage and the ball, we get an error in the measurement equal to $\pm 0.4 / \sqrt{2} \, \mathbf{mm} \approx \pm 0.3 \, \mathbf{mm} \, (\sqrt{0.3^2 + 0.3^2} \approx 0.4)$. This error is the size of a pixel.
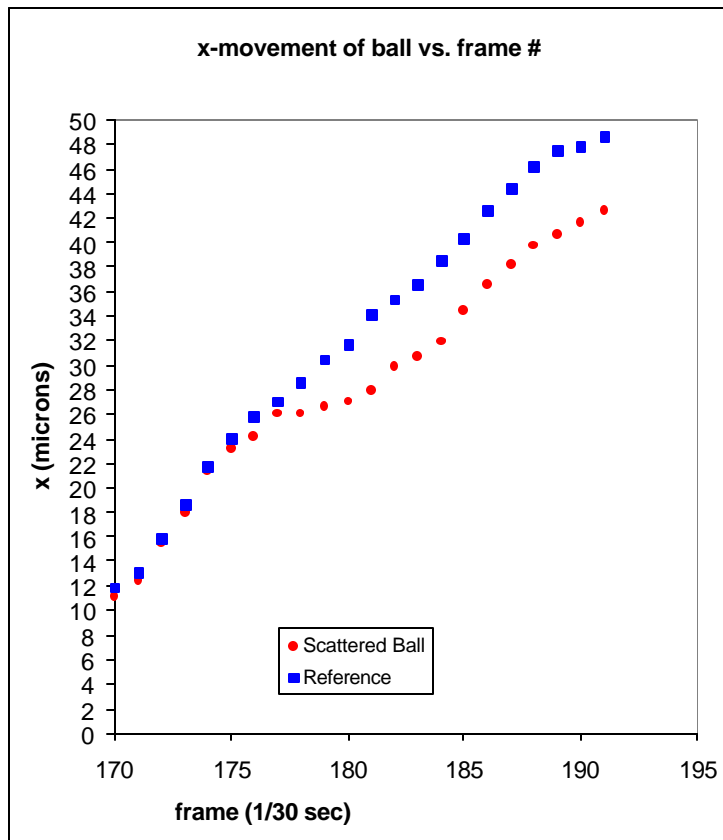
Figure 13: This plot shows the x positions of the ball and the reference point in the absolute reference frame (the reference frame of the laser trap) as a function of frame number. The motion of the ball mirrors the motion of the stage until after it is pulled into the trap (frame177) The ball almost comes to a standstill while it is in the trap (frames 177-178). As the ball leaves the trap and the viscous forces take over, the ball regains the speed of the stage (frame 182).

We then calculate the velocities of the ball and stage. Although the trap is small (~1μm in diameter) and the stage velocity is high (1.8μm/frame), the ball size is comparatively big (10μm in diameter). Hence, the ball should be in the trap for about 5 frames, which means that we can get the forces of the trap during this time. We determine the forces of the trap as a function of ball position using the equation ( ) detailed in the discussion on the viscous drag force.
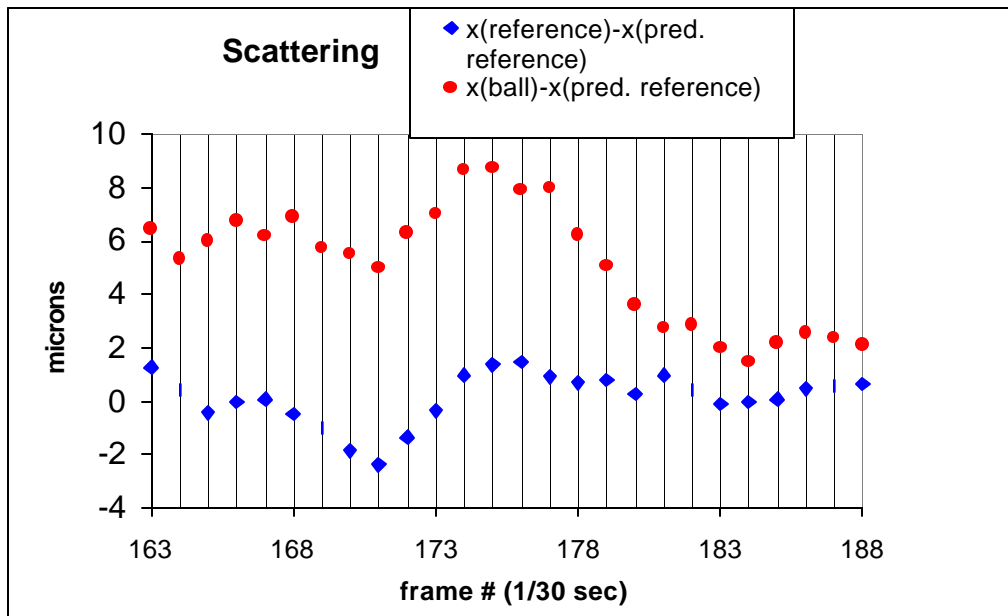

Figure 14: Subtracting away the average stage velocity uncovered some nonlinear behavior in the movement of the stage (in blue). Frames 167-175 show that this "hesitation" in the stage movement is also perpetuated in the movement of the ball: this means that the variation in this area is due to the stage. In red is the ball and in blue is the reference point.

2. Analysis

In order to determine what exactly is going on as the ball goes through the trap, we modeled the behavior in Excel and compared the results to the measured data. We solved the x and y coordinate positions simultaneously by an iterative formula to be explained below. A significant feature in to keep in mind is that the ball feels the y force before the x force. Our model accounts for the non-symmetric nature of our position curves. That is to say, the ball does not travel all the way through the trap along one coordinate axis: we never see the force increase and decrease along the same axis. We maintain that for this particular scattering event,
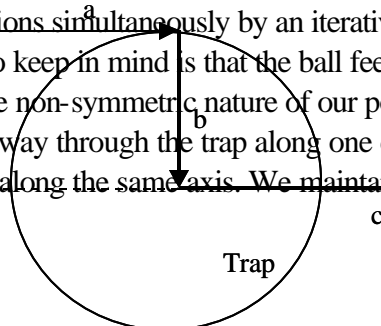
the ball is first pulled laterally to its initial direction of motion into the center of the trap (see figure…).

Figure   :Simplified diagram showing our understanding of the scattering event. In a first phase (a) the ball is incident on the trap at an impact parameter that we will call y_0. In a second phase (b), the ball is pulled into the trap by the attractive y forces. Finally the ball feels the resistive x forces as it is pulled out of the trap (c).

We derived our model from several key observations and measurements, which are crucial to the understanding of the behavior of the ball throughout the scattering event:

a) The velocity of the ball with respect to the stage and the fluid is always the terminal velocity because of the powerful viscous force (see section IV above).

b) There is a time delay between the times that the y position changes and the x velocity changes.

The model is as follows:

a) The initial position is $v_s(t_{frame} - t_{offset})x + y_0 y$ where v_s is the stage velocity, t_{frame} is the frame number and t_{offset} gives us an offset such that x=0 when the ball is at the center of the trap. The scattering parameter, the distance in the y direction from the center of the trap is y_0.

b) The fact that the ball is always at terminal velocity when it is moving relative to the stage gives us the force of the trap in the x and y directions:

$$F_{trap} = kre^{-\frac{r^2}{w_0^2}}$$

where k is the spring constant (a measurement of the strength of the trap), r is the coordinate in cylindrical coordinates ($r = \sqrt{x^2 + y^2}$) and w_0 is the radius of the trap.

c) The force contributes to the velocity of the ball for the next frame. In the x direction,

$$v_x = \frac{F_x t}{m_b} + v_s$$

In the y direction,

$$v_y = \frac{F_y t}{m_b}$$

d) The new position is $\overrightarrow{r_{i+1}} = \vec{r_i} + \vec{v_i}\Delta t$.

e) Iterating this gives us a predicted trajectory in the x and y directions.

f) The parameters are w_0, k, y_0 and t_{offset} . Varying these allows us to fit the model to the data (See figure below).
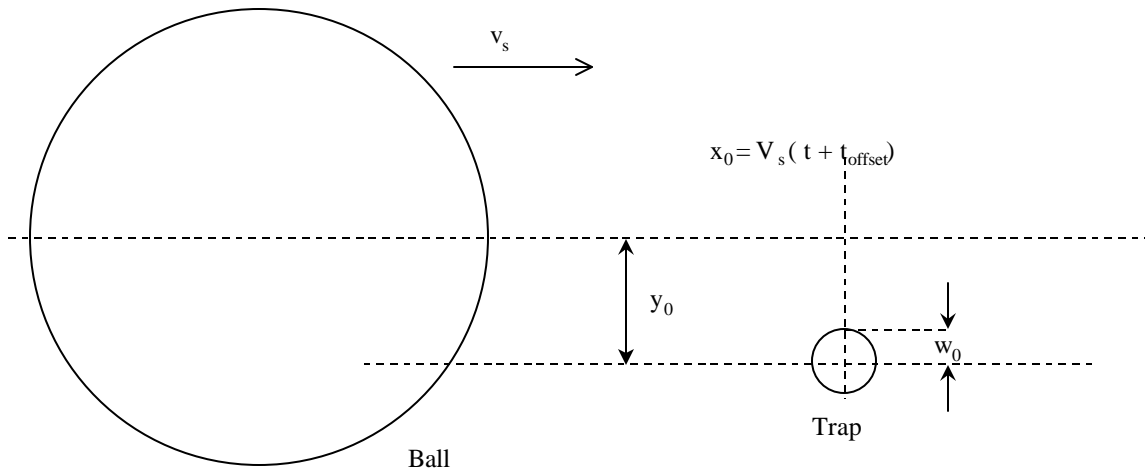
$$x_0 = V_s (t + t_{offset})$$

Figure : The relative sizes of the ball and the trap.

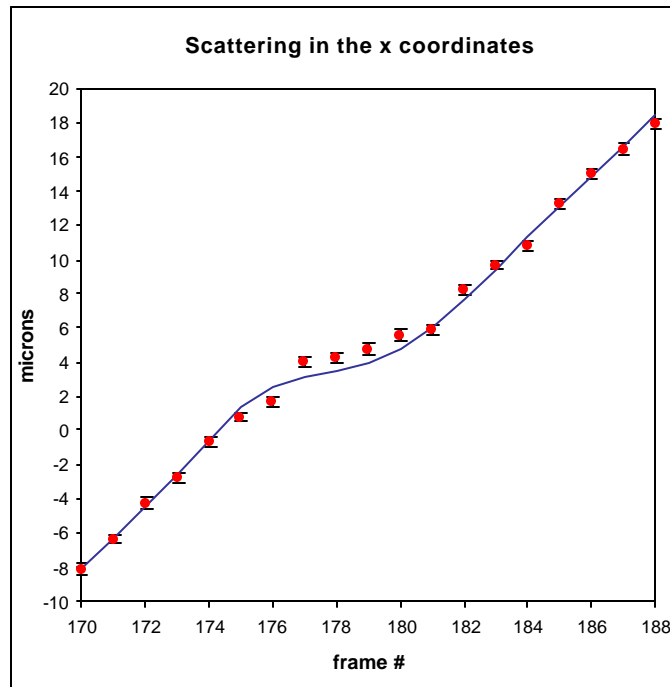The following figures show the model's fit to the data.

Figure : Plot showing the model's fit to the measured x coordinates of the ball (red points) in the reference frame of the trap, plotted versus the frame number (each frame is separated by 1/30 sec). The error in measurement is ± 0.3 microns. We could perhaps adjust parameters or even refine the model to better account for and fit the data when the ball is in the trap (frames 176-180). We corrected the measured x coordinates in order to eliminate the stage jitter by subtracting the coordinates of the reference point and adding back the predicted position of the stage.

Frame number	X(ball pred) (μm)	X (measured) (μm)	F (trap) (pN)	V_x (μm/frame)
170	-8.10	-8.10	0.00	1.80

171	-6.30	-6.32	0.03	1.81
172	-4.49	-4.24	0.22	1.88
173	-2.61	-2.78	0.59	2.01
174	-0.60	-0.69	0.39	1.94
175	1.34	0.77	-1.56	1.25
176	2.59	1.61	-3.57	0.54
177	3.12	4.01	-4.04	0.37
178	3.49	4.23	-3.69	0.50
179	3.99	4.76	-2.84	0.80
180	4.79	5.61	-1.57	1.24
181	6.03	5.83	-0.45	1.64
182	7.67	8.22	-0.05	1.78
183	9.46	9.69	0.00	1.80
184	11.26	10.84	0.00	1.80
185	13.06	13.23	0.00	1.80
186	14.86	15.01	0.00	1.80
187	16.66	16.47	0.00	1.80
188	18.46	17.93	0.00	1.80

Figure 16: Table showing the predicted x position, force, velocity of the ball for each frame (frames 170-188). For comparison, are the measured x values, which we corrected to account for the stage jitter: we subtracted the reference coordinates from the ball position point by point, then added the linear prediction for the stage position.
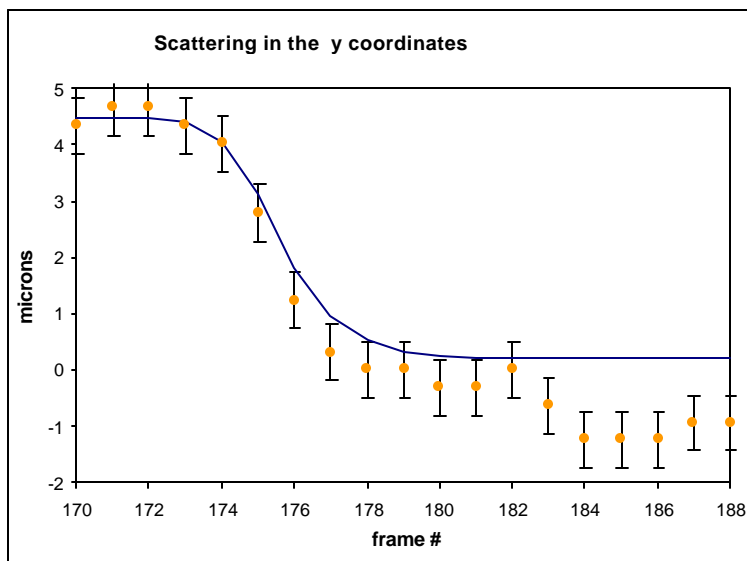

Figure 1: Plot showing the measured y position of the scattered ball with the best fit generated by the model. We simultaneously fit the x and y coordinates with the model so we could get a better fit by adjusting the parameters: then the fit for the x coordinates would suffer) Best fit of model to y coordinates of the scattered ball. The error in measurement is approximately ⊛0.5 microns. To get a better fit, we could increase the spring constant k, increase the trap size or decrease the scattering parameter y_0. In all three cases, however, a better fit for the y coordinates results in trapping in the x direction, which is contrary to what actually happens (see Appendix A). A possible explanation would be that the trap is asymmetric in the x and y directions as found by Paul Larson.

Frame	y(ball pred)	y (measured)	F (trap) (pN)	V_y (▪▪m/frame)

number	(μm)	(μm)		
170	4.50	4.34	0.00	0.00
171	4.50	4.65	-0.02	-0.01
172	4.49	4.65	-0.22	-0.08
173	4.41	4.34	-1.00	-0.35
174	4.06	4.03	-2.64	-0.93
175	3.13	2.79	-3.65	-1.29
176	1.84	1.24	-2.54	-0.90
177	0.94	0.31	-1.22	-0.43
178	0.51	0	-0.54	-0.19
179	0.32	0	-0.23	-0.08
180	0.24	-0.31	-0.08	-0.03
181	0.21	-0.31	-0.02	-0.01
182	0.21	0	0.00	0.00
183	0.21	-0.62	0.00	0.00
184	0.21	-1.24	0.00	0.00
185	0.21	-1.24	0.00	0.00
186	0.21	-1.24	0.00	0.00
187	0.21	-0.93	0.00	0.00
188	0.21	-0.93	0.00	0.00

Figure 17: Table showing the predicted y position, force, velocity of the ball for each frame (frames 170-188). For comparison, we include the measured y positions.
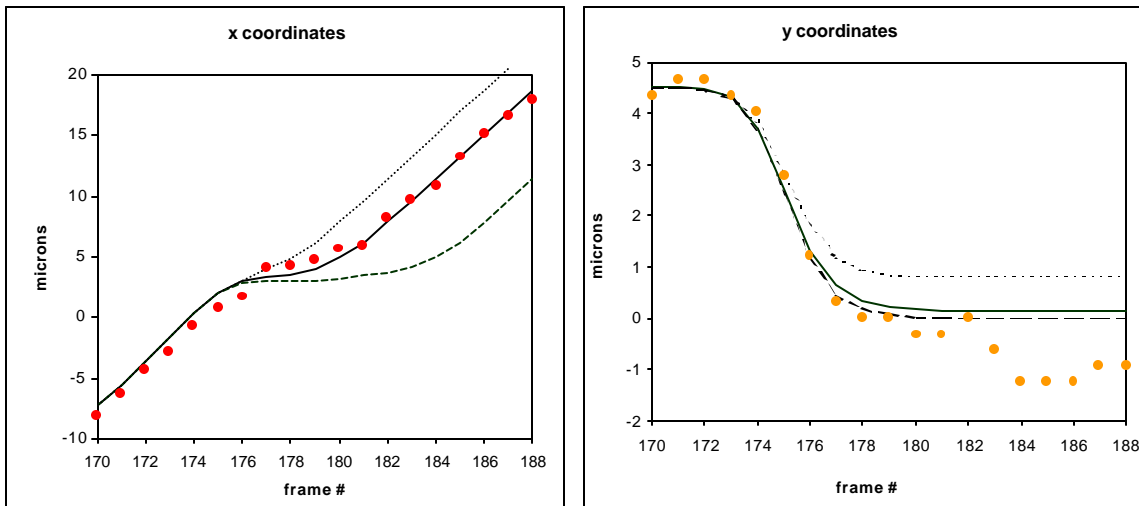

Figure : Plots showing minimum variations in spring constant parameter k for there to be a significant deviation from the x or y fitted curves. The best fit to the data is the solid line. To achieve a significant change, we increased k by approximately 5% (dashed line) and decreased k by approximately 11% (dotted line). Variations in the spring constant parameter are twice as sensitive when it is being decreased from the fitted value than when it is increased from the fitted value.
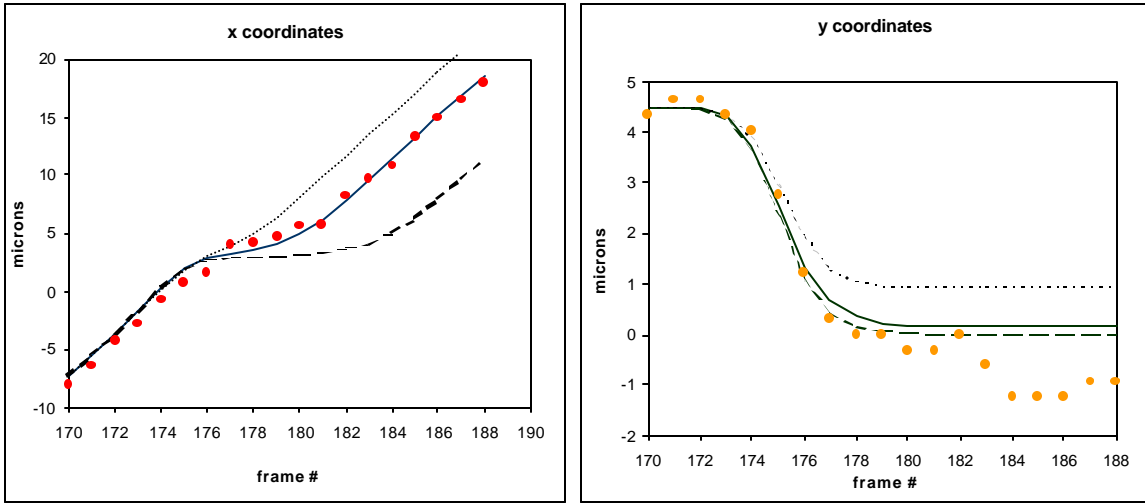
Figure   : Plots showing minimum variation in the trap radius parameter w_0 for there to be a significant change from the best fit to the x and y coordinates of the ball. The best fit of the model to the data is the solid line. Significant change occurs for a 1.5% increase in w_0 (dashed line) and for a 3.3% decrease in w_0 (dotted line). The modeled trajectory is twice as sensitive to decreases in the trap radius than increases in this parameter.
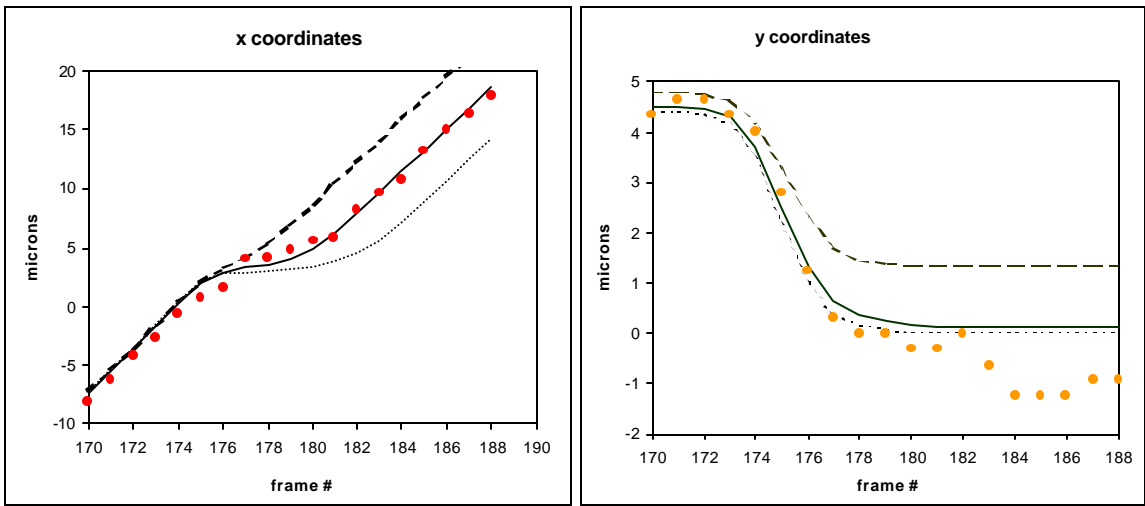

Figure   : Plots showing minimum variation in scattering parameter y_0 for there to be a significant deviation from the best fit to the x or y coordinates of the ball. The solid line is the best simultaneous fit to the x and y coordinates of the ball. Significant change occurs for a 7% increase in y_0 (dashed line) and for a 2% decrease in y_0 (dotted line). The model is approximately three times more sensitive to decreasing the scattering parameter than to increasing.
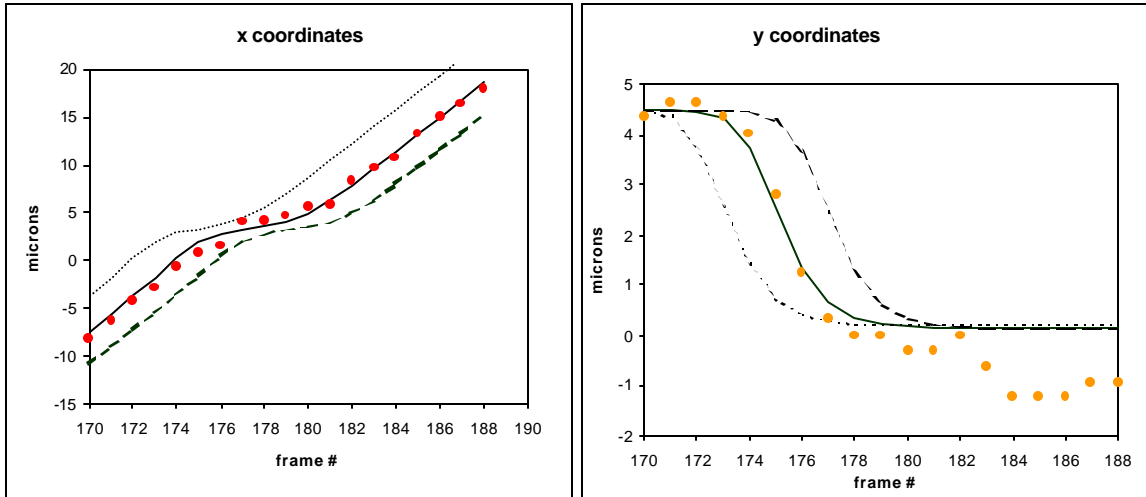
Figure : Plots showing minimum variation in the time offset parameter t_{offset} for there to be a significant deviation in the curves from the best fit. The line of best fit to the x and y coordinates simultaneously is a solid line. Varying this parameter gives us what we would expect. The curves are translated horizontally two frames to the left (dotted line) or to the right (dashed line) of the best fit.

IX. Conclusion

The experiment was much more successful than expected. We had anticipated measuring normal scattering, where we can only get one force measurement per scatter event. However, the experiment provides us with considerably more information. As the ball moves through the trap, we can actually determine the force on the ball for each position of the ball. This direct measurement of the forces of the trap was due to the viscous force. The trajectory changed much more than normal scattering because there is a strong viscous force: the ball is always at terminal velocity, which is the crucial fact that allows us to get the forces in the trap. This one scattering event, even marred by stage jitter, allows us to create a model for the forces, which can be used to fit to future data and even make predictions about the behavior of the trap given certain parameters.

We have observed and recorded two-dimensional scattering and have conducted the investigation into recording three-dimensional scattering. We have measured the forces of the trap in function of ball position to an accuracy of approximately 0.5pN in the x direction and 1pN in the y direction. We have obtained a position resolution of approximately 0.3 microns in the x direction and 0.5 microns in the y direction.

X. Future work

Now that we have a force model, we can make predictions and verify them experimentally. With a method of analysis in place, more data would allow us to gain further insight into the characteristics of the trap. For instance, we could try sending the ball through the trap along the y axis to better investigate the y forces. Pursuing this project into further depth, we could resolve the position of the ball with better accuracy. First of all, there appears to be a non-random error in the measurement of the y coordinates, which contributed to the

measurement error. This could be due to one of several possibilities: first of all, on retaking the data from the avi file, we found that the y fluctuation of the ball of approximately ※0.5 microns seemed to disappear. This suggests that it was error in measuring the coordinates. Alternatively, this feature could be real, the stage was "jiggling" in the y direction; however, the y coordinates of the stage do not seem to have the same fluctuation. Most probably then, it is an error in measurement: the reference point has a more pronounced edge that can be used as a "visual landmark" from frame to frame. With this in mind it would not be surprising if there were a more sizable measurement error in the ball's coordinates. The pixel size of 0.3 microns is apparently a limiting factor in the resolution of the ball's position. To achieve better position resolution, we could imagine transferring the data from the videocassette to a computer image file of higher pixel resolution: to avoid dropping frames in translation to the .avi format we could isolate and capture only those few frames of interest. Another obvious obstacle to achieving accurate data would be the stage translation: with smoother translation, a linear model would give us a much better approximation.

Analysis of further data will allow us to hone our model, we could obtain even more accurate force measurements. Taking and analyzing more data would hopefully clear up some of the apparently mysterious features in the current data. The strange step features in the y coordinates after we are assuming the ball is out of the trap, could be investigated. Varying the parameters of the model we can get some interesting features in this region such as oscillations in the y direction about the center of the trap. Further study will either refute this feature as an anomaly or prove it to be an important and interesting effect.

XI. Acknowledgements

Appendix A

---

[4] A. Ashkin. Forces of a single-beam gradient laser trap. In *Laser Tweezers in Cell Biology*, ed. M. P. Sheetz, 1-27, New York: Academic Press (1998).